DERIVING INTERVAL VELOCITIES FROM DOWNHOLE SEISMIC DATA

Erick Baziw

Baziw Consulting Engineers Ltd., Vancouver, Canada

Gerald Verbeek

Baziw Consulting Engineers Ltd., Vancouver, Canada

Keywords: Downhole seismic testing, seismic cone penetration testing, interval velocities, raypath refraction

ABSTRACT: When analyzing downhole seismic testing data in soil profiles with minimal variance in impedance between the various soil layers, the Straight Ray Assumption (SRA) methodology can be utilized to calculate interval velocities. However, source wave trajectories also adhere to Fermat's principle, which means that the raypath travels along the trajectory which requires minimum time between points. To properly account for this in soil profiles with significant variance in impedance between the soil various layers, the calculation of the interval velocities should no longer be based on the SRA methodology, but instead use the Iterative Forward Modeling (IFM) technique. This technique has many advantages over the SRA technique, such as: 1. The refraction of the raypath at layer boundaries is considered using Snell's Law. 2. Fermat's Principle of least time is adhered to. 3. Optimal interval velocity estimates are obtained by minimizing a cost function. 4. Extensive downhole time series measurement information (e.g., arrival times, cross-correlation time shifts, P-S wave time separation, and angles of incidence) can be taken into account within the cost function. 5. Measurement weights can be specified. 6. Slant ray raypaths are taken into account 7. The determination of meaningful error residuals for the evaluation of the accuracy of the estimated interval velocity. In this paper we will discuss the IFM technique to improve upon the SRA interval velocity estimates and demonstrate that the application of the IFM technique becomes even more essential in case of a soil profile with a top layer that has a relatively low interval velocity. The latter may also explain why according to some the use of downhole seismic testing is not appropriate for shallow depths.

1 INTRODUCTION

The ASTM standard (ASTM D7004 (2008)) for downhole seismic testing (DST) for site characterization assumes laterally homogeneous medium with possible transverse anisotropy. For laterally homogeneous medium, the downhole source wave travels through the stratigraphic profile and is refracted at layer boundaries as illustrated in Fig. 1 (Baziw (2002)). In this figure the angle θ_2 is called the angle of refraction and θ_1 the angle of incidence[1]. Equation (1) defines the relation between θ_1, θ_2, V_1 and V_2. This equation is referred to as *Snell's Law*[2] (Aki and Richards (2002)) and is derived from *Fermat's principle, which* states that a wave will take that raypath for which the travel time is stationary with respect to minor variations of the raypath (Baziw (2004a) and Shearer (1999)).

$$Sin\ \theta_1 / V_1 = Sin\ \theta_2 / V_2 = p \qquad (1)$$

In eq. (1) the quantity p is called the raypath parameter. In Fig. 1 and eq. 1, V_1 to V_{n+1} represent the consecutive vertices of the seismic ray as it travels from source to DST receiver. In eq. (1), if V_2 is less than V_1, then θ_2 is less than θ_1. However, when V_2 is greater than v_1, θ_2 increases to 90° when θ_1 reaches the critical angle. The critical angle, Θ, is defined as the angle where $\theta_2 = 90^\circ$ and the refracted wave (head wave) is travelling along the interface.

$$\Theta = Sin\ \theta_1 = Sin^{-1}\left(\frac{v_1}{v_2}\right) \qquad (2)$$

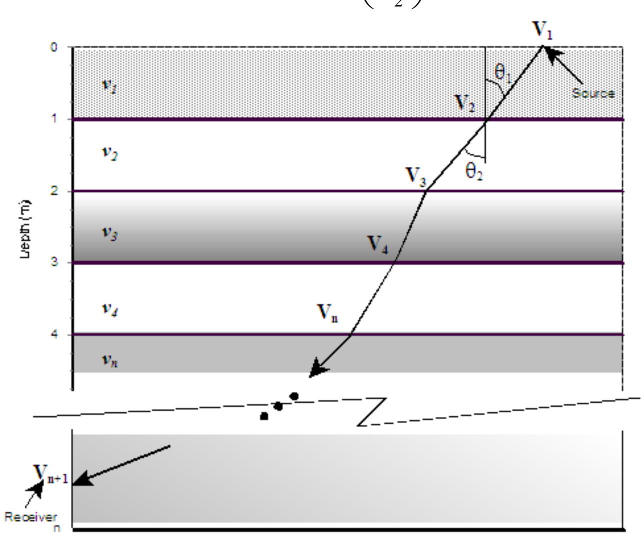

Figure 1. Refraction of a source wave as it travels from source to receiver

[1] Note: angle of reflection = θ_1.

[2] In optics, Snell's law is similarly used to describe the relationship between the angles of incidence and refraction when referring to light. In this case $Sin\ \theta_1 / Sin\,\theta_2 = V_1 / Vv_2 = n_2 / n_1$, where n_2 and n_1 are the refractive indices.

2 DERIVING INTERVAL VELOCITIES FROM DST DATA

The *Straight Ray Assumption* (*SRA*) methodology (Baziw (1993)) can be utilized to calculate interval velocities for stratigraphic profiles of minimal impedance mismatches. Referring to Fig. 2, the interval velocities from the SRA method are obtained by calculating the relative arrival time differences (e.g., $\Delta T = T_i - T_{i-1}$) between two successive depths z_i and z_{i-1} and by assuming straight ray travel paths from source to receiver when calculating travel path differences.

Example:

$$d_{i-1} = \sqrt{l_{i-1}^2 + z_{i-1}^2}, \qquad d_i = \sqrt{l_i^2 + z_i^2} \tag{3}$$

where z_{i-1} is the vertical depth of the seismic sensor package at interval index *i-1*, l_{i-1} is the source-sensor offset at interval index *i-1*, d_{i-1} is the travel distance of the source wave to interval index *i-1* assuming a straight ray trajectory, z_i is the vertical depth of the seismic sensor package at interval index *i*, l_i is the source-sensor offset at interval index *i*[3], d_I is the travel distance of the source wave to interval index *i* assuming a straight ray trajectory. The *SRA* interval velocity between depth increments *i-1* and *i* is then calculated from d_{i-1}, d_i, and the relative arrival time $\Delta T = T_i - T_{i-1}$, is given as

$$V_i = \frac{d_i - d_{i-1}}{\Delta T} \tag{4}$$

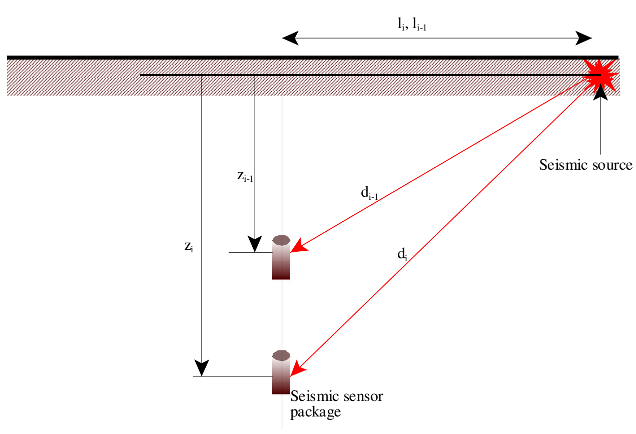

Figure 2. Schematic of the typical DST configuration.

A standard straight ray geometry assumes that the down going rays have spent an equal amount of time or have the same travel path within each interval layer as is shown in Fig. 3. The slant ray and refraction calculation take into account the time spent and corresponding travel path within each layer as illustrated in Fig. 3 (b)(e.g., D1, D2A and D3A within layer 1, D2B and D3B within layer 2 and D3C within layer C). The associated error in assuming a straight geometry as opposed to a slant ray or refraction geometry if there is significant impedance mismatches is significantly increased.

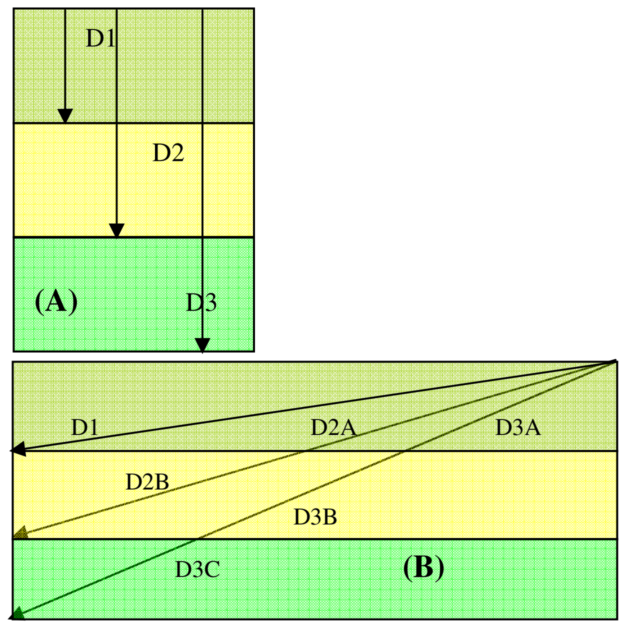

Figure 3. (a) Straight ray assumption. (b) Slant ray assumption.

For stratigraphic profiles of significant impedance mismatches or source radial offset the calculation of DST interval velocities should take into account the physics of refracting seismic waves (e.g., *Snell's Law* and *Fermat's Principle*) such as *Iterative Forward Modeling* (IFM) or *Data Inversion* (*DI*) (Baziw (2002)). These techniques have many advantages over the *SRA* technique, such as:

1. The refraction of the raypath at layer boundaries is considered using Snell's Law.
2. Fermat's Principle of least time is adhered to.
3. Optimal interval velocity estimates are obtained by minimizing a cost function.
4. Extensive downhole time series measurement information (e.g., arrival times, cross-correlation time shifts, P-S wave time separation, and angles of incidence) can be taken into account within the nonlinear cost function.
5. Measurement weights can be specified.
6. Variable interval velocity estimates can be accommodated so that comparisons or correlations can be made with other types of in-situ measurements.
7. The determination of meaningful error residuals for the evaluation of the accuracy of the estimated interval velocity.

[3] In general terms $l_i = l_{i-1}$ unless there is significant borehole deviation from vertical.

The ability of the IFM technique to improve upon the SRA interval velocity estimates depends on several DST site parameters such as radial seismic sensor - source offset, depth of interval velocity estimate, and variability of the *in-situ* velocity profile. Figure 4 (Baziw (2002) illustrates a simulated DST where the seismic source is radially offset from the seismic probe by 2.1 m, the seismic data capture starts at 1.5 m and goes to a depth of 7.5 m at one meter intervals.

Table 1 outlines the true interval velocities and the interval velocity estimates from the *IFM* technique with comparisons made to the *SRA* technique. As shown in Table 1, the IFM exactly recovered the true interval velocities and provided the source receiver ray paths illustrated in Fig. 1. The SRA interval velocity estimates did a poor job in estimating the true interval velocity estimates due to the site parameters specified being poorly conducive to a straight ray assumption.

Table 1. Comparing interval velocities (IVs) derived from IFM and those obtained from the straight ray assumption (Baziw (2002))

Interval Depth [m]	**Arrival Time [ms]**	**True IVs [m/s]**	**IFM IVs [m/s]**	**SRA IVs [m/s]**
0-1.5	22.98	112	112	112
1.5-2.5	24.26	181	181	536
2.5-3.5	27.31	209	209	267
3.5-4.5	36.96	101	101	94
4.5-5.5	40.70	214	214	246
5.5-6.5	44.54	232	232	246
6.5-7.5	55.12	128	128	126

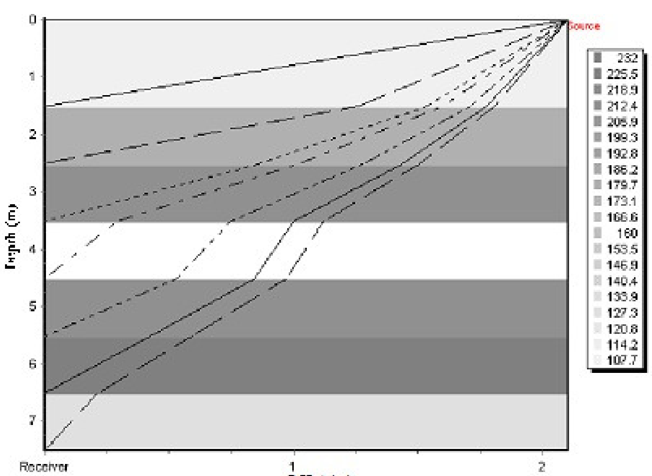

Figure 4.17: Specification of a seven layer variable velocity interval stratigraphic profile for comparing the performance of the IFM and SRA analysis techniques (Baziw (2002)).

The application of the IFM technique becomes even more essential in case of a soil profile with a top layer that has a relatively low interval velocity. In that case the arrival time in a deeper layer may occur prior to that in a shallower layer, as illustrated in Fig. 4 and Table 2, which lists the arrival times and the interval velocities obtained with the IFM technique.

It shall be obvious that in cases like this the use of the IFM technique is absolutely essential (e.g., for depth interval 0.5m to 2.5m the SRA would have given a negative interval velocity), and this may also explain why according to some the use of downhole seismic testing is not appropriate for shallow depths. It may well be that the applied data analysis method was not appropriate and that the Iterative Forward Modeling technique would have generated accurate results

Some investigators attempt to correct for the negative relative arrival times by multiplying the recorded arrival time by the cosine of the angle between the slant ray and the vertical, while utilizing the relative vertical travel distance. This technique is referred to as the vertical travel path correction (VTPC) and is illustrated in Fig. 5. In Fig. 5 the VTPC adjusted arrival time at depth Y_{D1} is calculated as $t1_{VPTC} = t1 \bullet \cos(\theta 1)$ and the VTPC adjusted arrival time at depth Y_{D2} is calculated as $t2_{VPTC} = t2 \bullet \cos(\theta 2)$. The interval velocity is then calculated as $V = (Y_{D2} - Y_{D1})/(t2_{VPTC} - t1_{VPTC})$. The validity of the VTPC is highly questionable and it appears to be more of an ad hoc approach. The VTPC does not take into account the true raypath of the source waves. In general terms, the VTPC assumes that we have a slant ray with no refraction. For example, the same corrections are applied irrespective of where the source wave crosses the interfaces.

Table 2. DST arrival times and associated IFM interval velocities.

Interval Depth [m]	**Arrival Time [ms]**	**IFM Interval Velocity Estimates [m/s]**
0-0.5	28.000	73.6
0.5-2.5	27.4555	134.1
2.5-3.5	33.5112	133.1
3.5-4.5	43.0900	97.3
4.5-5.5	51.4033	112.8
5.5-6.5	58.5370	131.6
6.5-7.5	66.2310	124.5
7.5-8.5	70.8411	201.4
8.5-9.5	75.8290	190.8

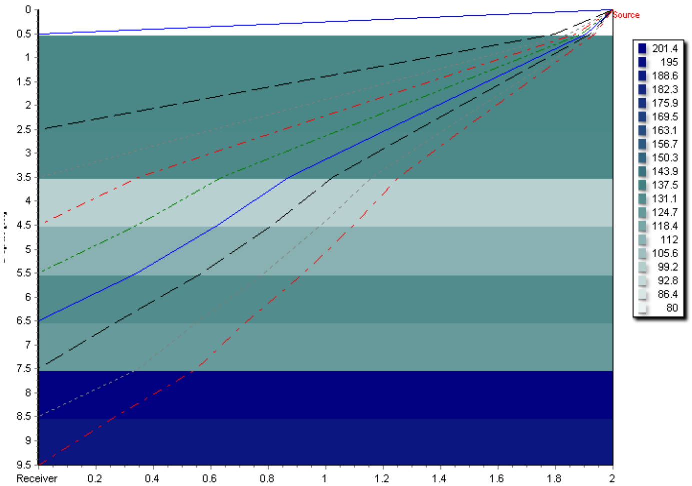

Figure 4.. Specification of an eight layer variable velocity interval stratigraphic profile to illustrate that the arrival time in a deeper layer can occur before that in the layer immediately above.

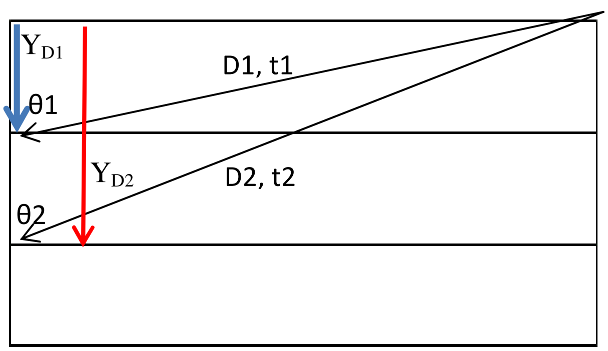

Figure 5. Schematic illustrating the variables within the VTPC technique.

There are in-situ conditions where there is significant near surface refraction (due to a very dense or very soft surface layer) and significant impedance mismatches with depth as illustrated in Fig. 6 and Table 3, which lists the arrival times and the interval velocities obtained with the IFM technique, the VTPC technique, and the SRA technique. Columns 1 and 2 of Table 3 outline the depth of data acquisition and corresponding arrival times for a simulated DST investigation The simulated arrival times reflect a dense surface layer overlying a soft soil, with below the soft soil intermixed soils of variable impedances. As can be seen from Table 3, the VTPC and SRA techniques would result in substantial errors in the estimated interval velocities, which demonstrates the necessity of using Snell's law for the true raypaths.

3 CASE STUDY

A case study is presented in this paper which outlines a DST carried out by IGEOTEST of Girona, Spain utilizing the seismic cone penetrometer ((Campanella et al. 1986 and Baziw (1993 and 2002)). This case study was selected due to the fact that there was a very dense surface layer overlying relatively softer soils (a very common condition).

The seismic cone penetration test (SCPT) utilized was a Baziw Consulting Engineers Ltd. SC system. A triaxial system configuration was implemented so that full waveform analysis could be carried out and the possibility of rod rotation could easily be taken into account. The sensors utilized were state-of-the-art fast response and high precision accelerometers (operational amplifier integrated into sensor) with bandwidths of 1 Hz to 10 KHz, range of ± 5 g and a resolution of 0.16 mg.

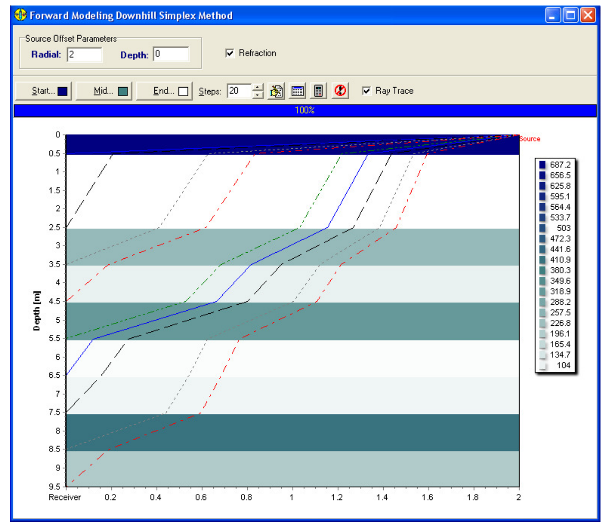

Figure 6. Source wave raypaths taking into account Snell's law for DST data outlined in columns1 and 2 in Table 3.

The seismic source was a horizontal shear (SH) hammer source. The SH source waves were generated at the outriggers which were positioned 1.5 metres from the centre of the rod strings (sensor-source radial offset). An electrical contact trigger was utilized. At each 1 m depth increment four sets of stacked data seismic cone time series (two on the right and two on the left side of the seismic probe) were generated and recorded. Each stack data trace consisted of averaging the seismic sensors' response to the two independent source generations.

Post signal processing consisted of applying a 10 Hz to 130 Hz 8thorder zero phase shift bandpass filter and cosine tapering bells to the recoded seismic data. In addition, time series data for the X and Y axes was rotated onto the full waveform axis utilizing a hodograms and polarization analysis (Baziw (2004a and 2004b)). This significantly simplified post analysis, because one is analysing one full waveform response as opposed to component responses on the X and Y axes. In addition, the implementation of polarization analysis significantly increases the signal to noise ratio because only the correlated responses on the X and Y axes are rotated onto the full waveform axis.

Table 3. Interval velocities for IFM/ VTPC/SRA techniques

Interval Depth (m)	Arrival Time (ms)	Modeled Interval Velocity (m/s)	IFM Interval Velocity Estimate (m/s)	VTPC Corrected Arrival Times (ms)	VTPC Interval Velocity Estimate (m/s)	VTPC Percent Error* (%)	SRA Interval Velocity Estimate (m/s)	SRA Percent Error* (%)
0-0.5	3	687.2	687.2	0.727607	687.2	0	687.2	0
0.5-2.5	30	73.3	73.3	23.42606	88.1	20.2	42.2	-42.4
2.5-3.5	34	241.8	241.8	29.52027	164.1	-32.1	207.4	-14.2
3.5-4.5	43.1	108.2	108.2	39.38528	101.4	-6.3	98.2	-9.2
4.5-5.5	46	319.1	319.1	43.2305	260.1	-18.5	320	0
5.5-6.5	58.5	79.1	79.1	55.91307	78.8	-0.3	75.9	-4.0
6.5-7.5	68.7	97.7	97.7	66.38034	95.5	-2.2	94.3	-3.5
7.5-8.5	70.9	412.3	412.3	69.01527	379.5	-8.0	440.9	6.9
8.5-9.5	75.8	199	199	74.17409	193.8	-2.6	199.2	0.1

*Percent error = (VTPC – true)x100/true or (SRA-true)x100/true

Figure 7 illustrates a vertical seismic profile (VSP) of the processed reversely polarized full waveforms for the acquired SCPT data.

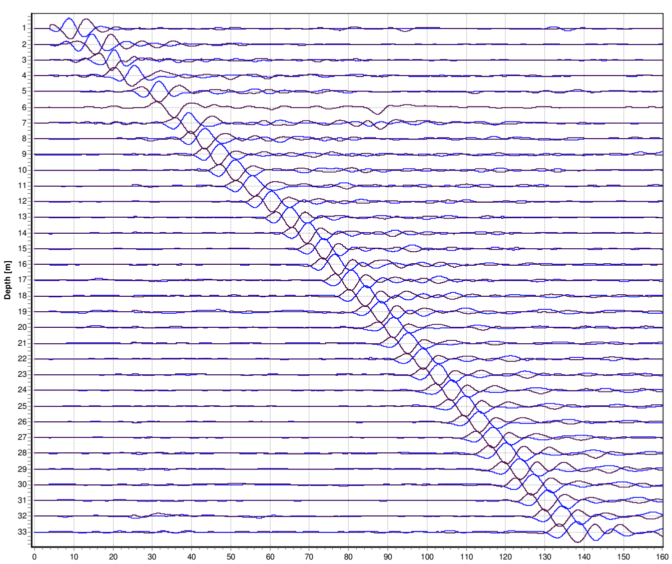

Figure 7. Processed reversely polarized full waveforms VSP.

The full waveform interval velocity estimates for this SCPT are summarized in Table 4 for the averaged crosscorrelation SRA estimates (right and left side (Baziw (1993 and 2002)) and the IFM estimate (Baziw (2002 and 2004a)). The percent difference between the SRA and IFM estimates is also shown in Table 4. The output of the IFM technique is illustrated in figure 8 where there is significant source wave refraction occurring at the 1 m interface due to the near surface high velocity layer. This near surface refraction results in significant near surface SRA interval velocity estimation error as indicated by the percentage difference in Table 4.

Table 4. SCPT interval velocity estimates.

Interval Depth [m]	Average Cross-correlation SRA Interval Velocity Estimate [m/s]	IFM Interval Velocity Estimate [m/s]	Percentage Difference (difference/average) x 100%
0-1	N/A	850	N/A
1-2	114	160	33.6
2-3	167	195	15.5
3-4	184	198	7.3
4-5	152	159	4.5
5-6	262	270	3
6-7	206	210	1.9
7-8	252	254	0.8
8-9	282	281	0.4
9-10	248	248	0
10-11	215	216	0.5
11-12	211	211	0.0
12-13	212	211	0.5
13-14	238	238	0.0
14-15	240	241	0.4
15-16	316	315	0.3
16-17	270	270	0.0
17-18	274	275	0.4
18-19	258	258	0
19-20	302	302	0
20-21	269	268	0.4

The results presented in this case study are more the rule than the exception. It is obvious that in cases like this the use of a IFM technique is absolutely essential and this may also explain why according to some the use of downhole seismic testing is not appropriate for shallow depths.

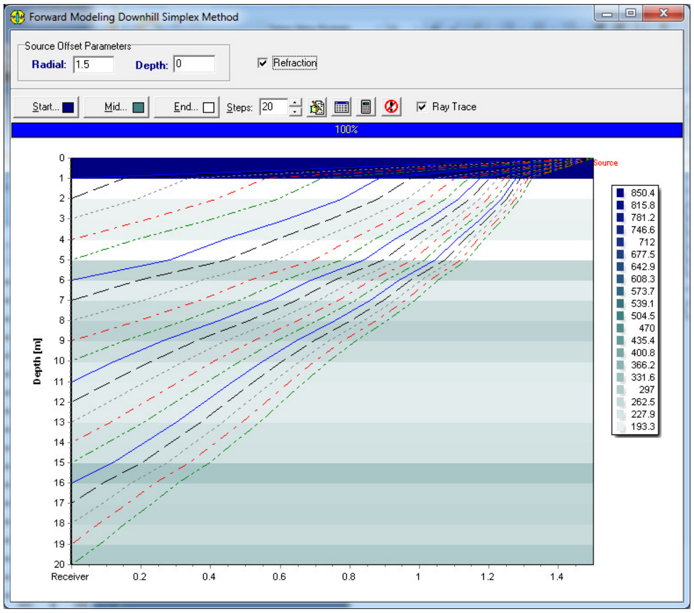

Figure 8. IFM output illustrating high velocity layer between 0 m to 1 m and significant near surface seismic ray refraction.

4 CONCLUSION

In downhole seismic testing (DST) there are *in-situ* conditions which require that raypath refractions governed by *Snell's Law* of refraction be taken into account when deriving interval velocities. Some important DST testing and *in-situ* conditions which effect interval velocity calculation errors when using the straight ray assumption (SRA) include sensor-source radial offset, in-situ impedance contrast and depth of seismic sensor. In general terms, it is desired to implement relatively large sensor-source radial offsets in order to minimize source noise (e.g., "rod noise" in seismic cone penetration testing). Alternatively, raypath refraction at large radial sensor-source offsets becomes a greater consideration for *in-situ* material which has significant impedance mismatches. Raypath refraction is more of a concern for shallow (5 times sensor-source radial offset) DST depths of analysis due to the fact that at deep DST investigations the source raypath is essential vertical. As was demonstrated in this paper *in-situ* layering which has significant impedance mismatches (e.g., slow layer overlying fast layer and vice-versa) can result in large errors in the interval velocity estimates if the SRA is implemented. For these reasons, it is in the authors' opinions that the implementation of *Snell's Law* of refraction must be taken into account when deriving interval velocities from DST data for depths which are less than 5 times the sensor-source radial offset.

REFERENCES

ASTM D7400 – 08. 2008. Standard Test Methods for Downhole Seismic Testing.

Baziw, E. 2002. Derivation of seismic cone interval velocities utilizing forward modelling and the downhill simplex method. Canadian Geotechnical Journal, 39: 1-12.

Aki, K. and Richards, P.G. 2002. Quantitative Seismology, 2nd edition, Sausalito, California: University Science Books. pp. 88-89.

Baziw, E. 2004a. Two and three dimensional imaging utilizing the seismic cone penetrometer. In Proceedings of the 2nd International Conference on Geotechnical Site Characterization (ISC-2), Porto, Portugal, 19-22 Sept. Millpress Science Publishers, 1611-1618.

Baziw, E., Nedilko, B, and Weir-Jones, I. 2004b. Microseismic Event Detection Kalman Filter: Derivation of the Noise Covariance Matrix and Automated First Break Determination for Accurate Source Location Estimation. Pure appl. geophys. Vol. 161, Number 2, 303-329.

Shearer, P.M. 1999. Introduction to Seismology, 1st edition,Cambridge: Cambridge University Press. pp. 328-354.

Baziw, E. 1993. Digital filtering techniques for interpreting seismic cone data. Journal of Geotechnical Engineering, ASCE, 119(6), 98-1018.

Campanella, R.G., Robertson, FTC and Gillespie, D. 1986.

Seismic cone penetration test. Proc. IN SITU86. ASCE, Geot. Spec. Publ. N o. 6, June: 116-130.